

MODELLING OPTICAL FIBRE CABLE

Optical fibre cables are made by placing optical fibres inside a loose tube packed with a water based gel, and then winding these loose tubes on to a central strength member in helically wound sections of alternating twist separated by reversing sections. The length of the loose tubes and their position on the strength member was modelled along with an analysis of where the optical fibres lie in the loose tubes.

1. Introduction

The topic was introduced by Mr Allan Davies, Engineering Manager for MM Cables Australia. A typical optical fibre cable is made in two stages: six optical fibres are enclosed by a loose fitting plastic tube, then six to twelve of these loose tubes are wrapped around a central strength member (CSM). These tubes are wrapped helically for a number of turns and then the rotation is reversed, so that reversal sections lie between helical sections of opposite rotation (see Figure 1 and Figure 2). The helical winding ensures that if the outer sheath of a loose tube is put under strain, the actual optical fibres themselves are not put under strain, provided the strain applied to the loose tube is not too great. Reversal of the helical winding is required not only for reasons connected with construction but also for reasons connected with installation. The strains that the cables experience can be due to tensions when being laid, and also to strains due to thermal expansion and contraction, since the cables have to be able to cope with ambient temperatures which can vary between -40°C and 70°C . An important concept is that of the strain free window, that is, the range of extension and contraction of the cable for which the optical fibres remain strain free. It is known that the strain free window is increased as the ratio of the length of helical sections to the length of the reversal sections is increased. For a given lay length, that is, the length along the CSM for one complete helical turn, the way to increase this ratio is to increase the number of turns in each helical section. However, this increases the amount of optical fibre and loose tube for a given length of CSM. It is clearly important to be able to model the reversal section accurately, since there is good evidence indicating that poor performance is associated with the reversal section.

Important questions for which answers are desired are:

1. How much optical fibre and how much loose tube is required to make a given length of cable?

2. Where is the loose tube laid on the CSM during manufacture?
3. When there is no tension on the cable, where do the fibres lie, especially in the reversal section?
4. Where do the fibres go when the cable is elongated under tension or compressed by low temperature?
5. Is there an optimal lay length and number of turns in the helical sections?
6. How tightly controlled does manufacturing have to be to comply with specifications?



Figure 1: Schematic diagram of the loose tubes wrapping around the central strength member. The wrapping starts off helically in an anticlockwise direction, then reverses to wrap clockwise.

2. Modelling the length of the loose tubes

The first problem to be investigated was the modelling of the length of a loose tube through a full cycle of a helical section, a reversal section, a reversed helical section and a further reversal section. A sequence of increasingly complicated models were investigated and compared with one particular sample of cable.

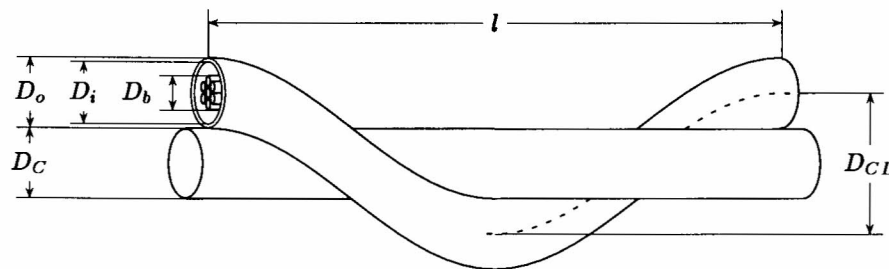


Figure 2: Helically stranded loose tube, showing dotted centre-line of the loose tube.

We denote by D_C the diameter of the CSM and by D_o the outside diameter of the loose tube. Then the centre-line of a loose tube is a curve on the surface of a cylinder of diameter $D_{CL} = D_C + D_o$ (see Figure 2). If θ and z are the standard polar coordinates for the surface of this cylinder, the curve representing the tube is defined once θ and z are given as piece-wise continuously differentiable functions of a suitable parameter.

In helical sections θ and z obviously satisfy

$$\theta - \theta_0 = \pm \frac{2\pi z}{l}$$

where the $+$ sign applies to right-handed (Z) twist, the $-$ sign applies to left-handed (S) twist sections, and l is the lay length (= pitch) of the helical windings (see Figure 2). A major problem is to know how to model the reversal sections. Two approaches were attempted:

1. Using geometrical models involving simple mathematical relations between θ and z .
2. Using a kinematic model based on the motion of the stranding machinery, that is, the actual machinery that winds the loose tubes on to the CSM.

2.1 Geometric modelling of the reversal section

Three simple curves were used by members of the group to model the reversal section. In all three cases we have that if N_P denotes the number of turns in each helical section and P is the length (along the CSM) of each complete cycle, then

$$P = 2(N_P l + 2\lambda), \quad (1)$$

where 2λ is the length of the reversal section.

1. The first curve considered was the one for which the θ - z relation in the reversal section is modelled by a quadratic equation in a way that ensures continuity of the tangent to the curve representing the loose tube. By a suitable choice of origin we may take the θ - z relation to be

$$\theta = \frac{\pi}{\lambda l} z^2. \quad (2)$$

Some basic geometry leads to the expression for the length L_T of tube per cycle,

$$L_T = 2N_P \sqrt{l^2 + \pi^2 D_{CL}^2} + \frac{4}{\lambda l} \int_0^\lambda \sqrt{\lambda^2 l^2 + \pi^2 z^2 D_{CL}^2} dz.$$

Straightforward integration yields

$$L_T = 2(N_P + \frac{\lambda}{l})\sqrt{l^2 + \pi^2 D_{CL}^2} + \frac{2\lambda l}{\pi D_{CL}} \sinh^{-1}(\frac{\pi D_{CL}}{l}). \quad (3)$$

2. In a second geometric model (G. Byrnes) the quadratic reversal section discussed above was replaced by the appropriate arc of a circle with half-angle $\phi = \tan^{-1}(\pi D_{CL}/l)$ and radius $\rho = \lambda/\sin\phi$. The expression for L_T then becomes

$$L_T = \left(2N_P + \frac{4\lambda}{\pi D_{CL}} \tan^{-1}(\frac{\pi D_{CL}}{l})\right) \sqrt{l^2 + \pi^2 D_{CL}^2}. \quad (4)$$

3. In the third geometric model (P-F. Siew) the quadratic reversal section was replaced by a cosine curve

$$\theta = \frac{2\lambda D_{CL}}{l} \left[1 - \cos\left(\frac{\pi z}{2\lambda}\right)\right]$$

which results in

$$L_T = 2N_P \sqrt{l^2 + \pi^2 D_{CL}^2} + 4 \int_0^\lambda \sqrt{1 + \frac{\pi^2 D_{CL}^2}{l^2} \sin^2\left(\frac{\pi z}{2\lambda}\right)} dz$$

yielding

$$L_T = 2N_P \sqrt{l^2 + \pi^2 D_{CL}^2} + \frac{8\lambda}{\pi} \sqrt{1 + \frac{\pi^2 D_{CL}^2}{l^2}} E\left(\frac{\pi}{2} \backslash \arctan(\pi D_{CL}/l)\right) \quad (5)$$

where $E\left(\frac{\pi}{2} \backslash \arctan(\pi D_{CL}/l)\right)$ is the complete elliptic integral of the second kind (see Abramowitz and Stegun, p. 590).

In many cases the dimensionless parameter $\zeta = \pi D_{CL}/l$ is a small quantity (e.g. for the sample cable $\zeta \approx 0.225$). It is interesting to note that, correct to terms of order ζ^4 , equations (3), (4) and (5) respectively are

$$L_T = 2N_P \sqrt{l^2 + \pi^2 D_{CL}^2} + 4\lambda \left[1 + \frac{1}{6}\zeta^2 - \frac{1}{40}\zeta^4 + O(\zeta^6)\right], \quad (6)$$

$$L_T = 2N_P \sqrt{l^2 + \pi^2 D_{CL}^2} + 4\lambda \left[1 + \frac{1}{6}\zeta^2 - \frac{11}{120}\zeta^4 + O(\zeta^6)\right] \quad (7)$$

and

$$L_T = 2N_P \sqrt{l^2 + \pi^2 D_{CL}^2} + 4\lambda \left[1 + \frac{1}{8}\zeta^2 - \frac{3}{64}\zeta^4 + O(\zeta^6)\right], \quad (8)$$

showing the essential robustness of these simple geometrical models.

Now consider the sample cable. This has $D_{CL} = 5.65$ mm, $P/2 = 720$ mm and $l = 79$ mm. If we take $N_P = 6$, the nominal number of turns between reversals, then from equation (1) we find that $\lambda = 123$ mm. Entering these values into equation (3) or equation (4), we obtain $L_T/2 = 734$ mm, for a length difference $(L_T - P)/2$ per half cycle of 14 mm. Equation (5) similarly gives $L_T/2 = 733$ mm for a length difference per half cycle of 13 mm. Both of these are slightly high when compared with the value 10.5 mm obtained by measuring the actual cable.

The number N_P allows some tuning of the model, since it is not clear quite where the helical section can be said to end and the reversal section begin. If we set $N_P = 4$ for the above cable, the first rotation at each end of the “helical” section is taken to be part of the reversal. This is borne out somewhat by the fact that the pitch of this winding is measurably longer than the others. Corresponding to $N_P = 4$ we have $\lambda = 202$ mm. Entering these new values into equation (3) or equation (4) we obtain $L_T/2 = 731$ mm and we find that equation (5) gives $L_T/2 = 730$ mm, all of which are in in better agreement with measurement.

However, the real problem that we would like to address is, given the draw speed of the cable, the number of turns that are completed by the stranding machine before a reversal is begun, and the angular velocity of the stranding machine as a function of the time, to determine the length of loose tube used as well as its location around the CSM.

2.2 Kinematic modelling of the reversal section

As a function of the time t , the stranding machinery has an angular velocity $\omega(t)$ of the form given in Figure 3. As a first approach to using this information, the problem was modelled (P-F. Siew, S. Lord) by making the assumption that

$$\frac{d\theta}{dt} = \omega(t) \quad (9)$$

$$\frac{dz}{dt} = V, \quad (10)$$

where, as before, θ and z are cylindrical polar coordinates and V is the draw speed of the cable. It is convenient to use the notation

$$T_n = \sum_{i=1}^n t_i. \quad (11)$$

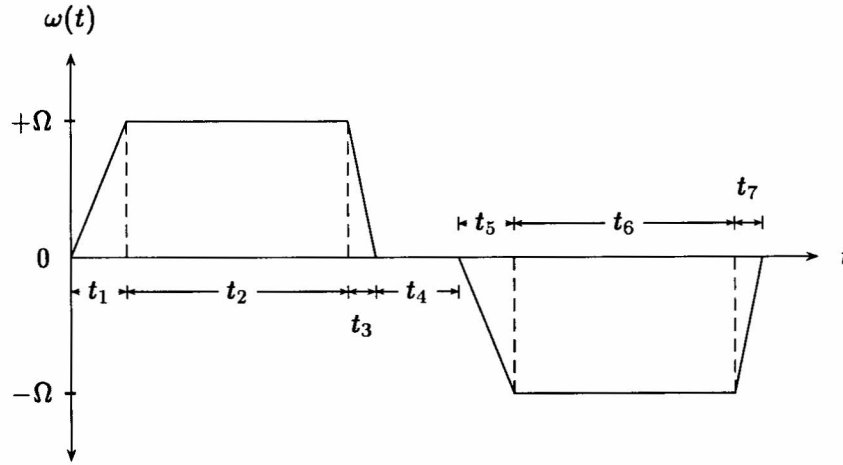


Figure 3: Angular velocity of the stranding machine. Note that $t_5 = t_1$ and $t_7 = t_3$.

We find that the angular velocity $\omega(t)$ is given by

$$\omega(t) = \begin{cases} \Omega t/t_1 & 0 \leq t \leq T_1, \\ \Omega & T_1 \leq t \leq T_2, \\ \Omega [1 - (t - T_2)/t_3] & T_2 \leq t \leq T_3, \\ 0 & T_3 \leq t \leq T_4. \end{cases}$$

The arc length s is given as a function of the time t as

$$s(t) = \int_0^t \sqrt{V^2 + \frac{D_{CL}^2 \omega(t')^2}{4}} dt'.$$

If we write $k_1 = D_{CL}\Omega/(2Vt_1)$, $k_2 = V\sqrt{1 + (D_{CL}\Omega/(2V))^2}$ and also $k_3 = D_{CL}\Omega/(2Vt_3)$, and if we introduce the function $f(k, T, t)$ defined by

$$f(k, T, t) = \frac{V}{2} \left[(t - T) \sqrt{1 + k^2(t - T)^2} + \frac{1}{k} \sinh^{-1}(k(t - T)) \right] \quad (12)$$

we find that $s(t)$ is given by

$$s(t) = \begin{cases} f(k_1, 0, t), & 0 \leq t \leq T_1, \\ f(k_1, 0, T_1) + k_2(t - T_1), & T_1 \leq t \leq T_2, \\ f(k_1, 0, T_1) + k_2 t_2 + f(k_3, T_2, t), & T_2 \leq t \leq T_3, \\ f(k_1, 0, T_1) + k_2 t_2 + f(k_3, T_2, T_3) + V(t - T_3), & T_3 \leq t \leq T_4. \end{cases}$$

For the cable being considered which has a cable length of 1440 mm for a full cycle, we obtain an excess length of 29.0 mm, corresponding to a fractional increase of 2.01%.

One problem with this model is that it implies that the loose tubes are straight in part of the reversal section, and this is not borne out by observation of the manufactured cable. Furthermore, from the data presented, it was noted that the number of complete helical turns actually obtained on the cable differed from the number that the stranding machine is set to give, which suggests that there is a lag or advance factor which is probably a function of the inertia of the system, the stiffness of the loose tube and the friction between the loose tubes and the CSM. The influence of these factors has not been modelled in the above treatment.

A partial explanation for the difference between the the number of turns actually laid down on the CSM and the number of turns preset on the stranding machine was given by N. Zoubtchenko. He reasoned that in the process of laying down the loose tubes on the CSM there is an important geometrical consideration, which may be illustrated with reference to Figure 4.

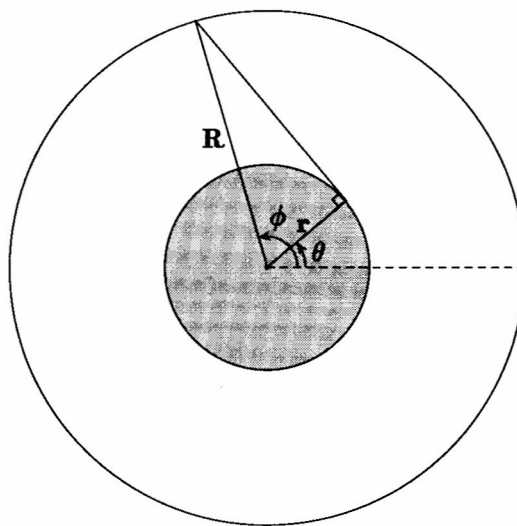


Figure 4: The coordinate setup of the cable twisting.

If ϕ is the angular coordinate of the hole in the strander wheel through which one of the loose tubes is being supplied, and if θ is the angular coordinate on the point on the CSM at which this tube makes contact, then it is only true that $\dot{\theta} = \dot{\phi}$ so long as $\dot{\phi}$ is one-signed, which for convenience we will assume is positive. As soon as $\dot{\phi} = 0$, i.e. as soon as ϕ achieves a maximum, θ remains constant until ϕ has rotated back through an angle 2γ , where $\gamma = \cos^{-1}(D_{CL}/D)$, where D is the diameter of the circle of holes in the strander wheel. Zoubtchenko is currently modelling this process in more detail.

3. The strain free window (G. Byrnes)

Consider the situation of a bundle of fibres running inside a loose tube. In the case where the fibre length is exactly equal to that of the tube, we can assume the bundle of fibres and the tube to be concentric (see Figure 2). If the tube is now strained, so that the fibres are shorter than the centre-line of the tube, the fibres must either lie along a path inside the tube whose length is equal to that of the unstrained fibres, or the fibres must strain. The straining of the fibres is unavoidable if the tube is straight, and in this case the optical attenuation in the fibres will increase to unacceptable levels.

In a cable where the tubes are wound around a central member, the curvature of the tube makes it possible for the fibres to find a shorter path than the centre-line of the loose tube and thereby avoid an increase in attenuation. We will simplify the problem by making the approximation, common in the cable industry, of treating a bundle of n fibres, each of diameter D_f , as a single fibre with diameter given by the approximate formula

$$D_b = D_f \sqrt{\frac{5n-2}{3}}.$$

Then since this bundle runs in a tube with internal diameter D_i , we replace this with a line running inside a tube of diameter $D_{eff} = D_i - D_b$.

In the case of a helix, the difference between the centre-line and shortest lengths can be calculated exactly. For a helix of radius a and lay length l , the arc-length of one revolution of the helix is given by

$$\sqrt{l^2 + 4\pi^2 a^2}.$$

The shortest path inside the tube runs along the inside surface closest to the central axis of the helix. This curve is itself a helix: the centre-line is a helix of radius $D_{CL}/2$, while the shortest path has radius $(D_{CL} - D_{eff})/2$. Thus the relative change is given by

$$\Delta_H = \frac{\sqrt{l^2 + \pi^2 D_{CL}^2} - \sqrt{l^2 + \pi^2 (D_{CL} - D_{eff})^2}}{\sqrt{l^2 + \pi^2 D_{CL}^2}}.$$

For a cable with $n = 6$, $D_f = 0.25$ mm (including coating), $D_{CL} = 5.65$ mm, $l = 79$ mm and $D_i = 1.6$ mm, we find $D_{eff} = 0.836$ mm and hence $\Delta_H = 0.66\%$.

While there is no exact expression for the shortest path through the reversal section, we can still obtain an expression for the relative change in path length accurate to first order. Note that to shorten a curve as much as possible for

a given perturbation, it should be displaced in the direction of the principal normal vector \mathbf{N} to the curve, given by

$$\mathbf{N} = \frac{d}{ds} \mathbf{T},$$

where \mathbf{T} is the unit tangent to the curve and s is the arc-length. The modulus of \mathbf{N} is called the curvature, denoted by κ , with $\kappa = |\mathbf{N}| = 1/\rho$, where ρ is the radius of curvature. Note that in general ρ is non-constant. Note also that the relative change in the arc-length of a curve which has been displaced in the direction \mathbf{N} by an amount $\epsilon(z)$ is, to first order,

$$\frac{1}{L} \int_0^L \frac{\epsilon(z)}{\rho(z)} dz = \frac{1}{L} \int_0^L \epsilon(z) \kappa(z) dz,$$

where L is the arc-length of the curve.

Now when looking for the shortest path inside a tube, we have $\epsilon(z) = D_{eff}/2$ constant, since we can only move from the centre to the inside wall of the tube. Thus for a tube following an arbitrary curve C , the relative change in length from centre to shortest path is approximately

$$\Delta_C = \frac{1}{2} K D_{eff},$$

where K is the average curvature along the path.

For the quadratic model of the tube path, it should be noted that κ is not continuous across the joins between the helical and parabolic sections. However this should not introduce significant error.

For a curve on the surface of a cylinder of radius a , with position vector in cartesian coordinates, we have

$$\mathbf{r}(z) = (a \cos \theta(z), a \sin \theta(z), z).$$

The corresponding unit tangent vector is given by

$$\mathbf{T} = \left(\frac{-a \sin \theta(z)}{(1 + a^2 \theta'^2)^{1/2}}, \frac{a \cos \theta(z)}{(1 + a^2 \theta'^2)^{1/2}}, \frac{1}{(1 + a^2 \theta'^2)^{1/2}} \right),$$

where $\theta' = d\theta/dz$. We then have $\kappa = |\mathbf{N}|$, where

$$\mathbf{N} = \frac{1}{(1 + a^2 \theta'^2)^{1/2}} \frac{d\mathbf{T}}{dz}.$$

A tedious calculation then gives

$$\kappa = \frac{a}{(1 + a^2 \theta'^2)^{3/2}} \left\{ \theta''^2 + (1 + a^2 \theta'^2) \theta'^4 \right\}^{1/2}.$$

For the helical sections this is simply

$$\kappa_H(z) = \frac{2\pi^2 D_{CL}}{l^2 + \pi^2 D_{CL}^2},$$

which for the cable parameters above yields $\rho_H = 1/\kappa_H = 58.8$ mm. The calculated relative path length change using this is $\frac{1}{2} \times 0.836/58.8 = 0.71\%$, not too far from the exact value of 0.66%.

For the case of the reversal section of the quadratic model, we find that

$$\kappa_Q(z) = \frac{a}{\left(1 + \frac{\pi^2 D_{CL}^2}{\lambda^2 l^2} z^2\right)^{3/2}} \left\{ \frac{4\pi^2}{\lambda^2 l^2} + \left(1 + \frac{\pi^2 D_{CL}^2}{\lambda^2 l^2} z^2\right) \frac{16\pi^4 z^4}{\lambda^4 l^4} \right\}^{1/2}.$$

The relative change for the complete quadratic model may be found from

$$\Delta_Q = \frac{6.6 \times 10^{-3} N_P l + D_{eff} \int_0^\lambda \kappa_Q(z) dz}{N_P l + 2\lambda}.$$

For the values $N_P = 6$, $\lambda = 129$ mm and $l = 79$ mm we find that

$$\int_0^\lambda \kappa_Q(z) dz = 0.789,$$

which results in $\Delta_Q = 0.53\%$, showing a substantial reduction in the strain free window. If we use the values $N_P = 4$, $\lambda = 202$ mm and $l = 79$ mm we find that

$$\int_0^\lambda \kappa_Q(z) dz = 1.231,$$

giving an even worse strain free window of $\Delta_Q = 0.43\%$. This clearly shows the importance of having a long helical section compared with the length of the reversing section.

4. Discussion

Two outstanding problems remain, namely, (1) to develop a detailed dynamically based model for the way in which the stranding machine lays the loose tubes on to the central strength member, and (2) to investigate the helical buckling modes of the optical fibres inside the loose tubes. As well as including the effect of the stiffness of the loose tubes, the first problem needs to take into account the fact that the binding tapes, which ultimately fix the location of the loose tubes on the CSM, are layed down in a preferential direction on the cable. Investigation of the second problem will need to be both experimental and theoretical (see Thompson and Champneys, 1996), but will need to go beyond this work in order to take into account the effect of the optical cable touching the inside wall of the loose tube.

Acknowledgements

This problem was co-moderated by Barrie Fraser and Ted Fackerell. We are grateful to Allan Davies and Kate McKeand from MM Cables for their readiness at all times to answer our questions, to Peg-Foo Siew for a Maple program to calculate the length of the loose tube in Section (2.2), and to Jim Clark for the diagrams. The problem was attended by Graham Byrnes, Jim Clark, Allan Davies, Vincent Hart, Stephen Lord, Kate McKeand, Bernhard H. Neumann, Peg-Foo Siew, Anthony Stace, Dave Stump, Phil Unterberger and Nikolai Zoubtchenko.

References

- M. Abramowitz and I.A. Stegun, (Eds) *Handbook of Mathematical Functions* (Dover Publications, NY, 1970).
- J.M.T. Thompson and A.R. Champneys, "From helix to localized writhing in the torsional post-buckling of elastic rods", *Proc. R. Soc. Lond.* A452 (1996), 117–138.